

contact tunnel diodes. By these arguments it is seen that for most high-frequency diode calculations the correction need not be applied. Similar arguments apply when the spreading resistance with skin effect is being considered in a transistor. While the resistivity of the transistor material may be one to two orders of magnitude higher than in a microwave diode, the frequency of operation is usually two to three orders of magnitude less than the 100 GHz figure used here. Again the correction term should prove negligible.

IV. CONCLUSIONS

Equations for the spreading resistance of the broad area variable-capacitance diode and the point-contact variable-resistance diode have been derived in terms of frequency, material characteristics (μ , ϵ , σ), and physical parameters (b/a) and (w/a). The results are presented in (37) and (68).

The field equations for the point-contact diode configuration have been derived in terms of the oblate spheroidal coordinates. It has been shown that this is the natural coordinate system for such an analysis and that the spreading resistance is quite readily derived in this system.

A discussion is presented which shows that the effects of displacement current in the semiconductor are, in most instances, negligible in comparison to the conduction currents.

REFERENCES

- [1] R. W. P. King, *Electromagnetic Engineering*. New York: McGraw-Hill, 1945.
- [2] L. E. Dickens, "Spreading resistance as a function of geometry" (to be published). Both papers based on Tech. Rept. NAS-1, prepared for NASA/GSFC under Contract NAS 5-3546, and Tech. Doc. Rept. AL-TDR-64-240, prepared for AFAL/RTD under Contract AF 33(657)-11029.
- [3] R. Holm, *Electric Contacts*. Stockholm: Hugo Gebers Forlag, 1946.
- [4] J. A. Stratton, *Electromagnetic Theory*. New York: McGraw-Hill, 1941.
- [5] E. Jahnke and F. Emde, *Tables of Functions*. New York: Dover, 1945.
- [6] L. A. Blackwell and K. L. Kotzebue, *Semiconductor-Diode Parametric Amplifiers*. Englewood Cliffs, N. J.: Prentice-Hall, 1961.
- [7] K. K. N. Chang, *Parametric and Tunnel Diodes*. Englewood Cliffs, N. J. Prentice-Hall, 1964.
- [8] H. C. Torrey and C. A. Whitmer, *Crystal Rectifiers*. New York: McGraw-Hill, 1948.
- [9] C. Flammer, *Spheroidal Wave Functions*, A Stanford Research Inst. Monograph. Stanford, Calif.: Stanford University Press, 1957.
- [10] G. A. Korn and T. M. Korn, *Mathematical Handbook for Scientists and Engineers*. New York: McGraw-Hill, 1961.
- [11] M. E. Hines, "High frequency limitations of solid-state devices and circuits," a Discourse presented to the International Solid-State Circuits Conference, Univ. of Pa., Philadelphia, 1963.
- [12] W. M. Sharpless, "Gallium-arsenide point-contact diodes," *IRE Trans. on Microwave Theory and Techniques*, vol. MTT-9, pp. 6-10, January 1961.

An Exact Calculation for a T-Junction of Rectangular Waveguides Having Arbitrary Cross Sections

EUGENE D. SHARP, MEMBER, IEEE

Abstract—An exact method is developed for the calculation of the electrical performance of the rectangular waveguide T-junction. This method is used to find the equivalent circuit of a rectangular waveguide T-junction in which both cross-sectional dimensions of the side waveguide are different from the cross-sectional dimensions of the through waveguide. The theoretical calculations for a particular T-junction of this type are verified by experimental measurements. In this method the electrical performance is analyzed by using equivalent-circuit concepts applied to waveguide modes to calculate an admittance matrix relating propagating and cutoff waveguide modes to each other. Then the cutoff modes are terminated in their characteristic impedance, and an equivalent admittance matrix of the junction is found relating only the propagating modes in each waveguide to each other. The analysis is valid when any number of

modes can propagate in the waveguides forming the junction. The inversion of an infinite matrix is required; however, any desired accuracy can be obtained by considering a matrix of finite but sufficient size or equivalently by considering a sufficient number of cutoff modes.

I. INTRODUCTION

IN THE PAST few years, interest has been shown in waveguide filters that employ waveguides operating below cutoff. Experimental data have been published giving the performance of a reactive filter consisting of an *E*-plane T-junction in which the side waveguide of the junction is of a smaller cross section than the through waveguide [1]. The side arm is short circuited a distance from the junction. This structure acts as a narrowband reject filter with the rejection band centered just above the side waveguide cutoff frequency.

The same type junction has been used in waveguide low-pass dissipative filters. Instead of being short circuited, the

Manuscript received March 25, 1966; revised September 30, 1966. The work reported in this paper was performed while the author was at Stanford Research Institute and was reported in a Technical Note for Rome Air Development Center, Rome, N. Y.

The author is with TRG-West, Incorporated, Menlo Park, Calif., a subsidiary of Control Data Corporation.

side waveguide is terminated in a matched load, and many side waveguides are connected to the through waveguide. At frequencies below the cutoff frequency of the side waveguides, the power is passed through the filter with small attenuation. At frequencies above the cutoff frequency of the side waveguides, power is coupled into the side waveguides and dissipated in the loads. Experimental data on the low-pass dissipative filter are available [2]-[4].

A calculation of the electrical performance of the junction used in the filters is presented in this paper. A sketch of such a junction is shown in Fig. 1.

It is well known that the electric and magnetic fields inside an ideal waveguide with infinitely conducting walls can be expanded in an infinite series of the waveguide mode functions as follows [5]:

$$E(x, y, z) = \sum_n v_n(z) E_{tn}(x, y) + i_n(z) E_{zn}(x, y)$$

$$H(x, y, z) = \sum_n i_n(z) H_{tn}(x, y) + v_n(z) H_{zn}(x, y) \quad (1)$$

where $E(x, y, z)$ is the electric field in the waveguide, $H(x, y, z)$ is the magnetic field in the waveguide, and $v_n(z)$, $i_n(z)$ are the equivalent voltage and current, respectively, giving the field variations along the longitudinal dimension z . The waveguide mode functions obey the following orthogonality relationships:

$$\int_S E_{tm} \cdot E_{tn} dS = \int_S H_{tm} \cdot H_{tn} dS = \delta_{mn}$$

$$\int_S E_{zm} \cdot E_{zn} dS = -\frac{k_{cn}^2}{k^2} Z_0^2 \delta_{mn}, \quad \delta_{mn} = 1 \quad \text{if } m = n$$

$$\int_S H_{zm} \cdot H_{zn} dS = -\frac{k_{cn}^2}{k^2} Y_0^2 \delta_{mn}, \quad \delta_{mn} = 0 \quad \text{if } m \neq n \quad (2)$$

where the integrals are taken over the waveguide cross section. The characteristic wave impedance Z_{wn} and the phase constant β_n of the n th waveguide mode are defined to be

$$Z_{wn} = Z_0 \begin{cases} k/\beta_n \\ \beta_n/k \end{cases}$$

$$\beta_n = (k^2 - k_{cn}^2)^{1/2} \quad (\text{for propagating modes})$$

$$\beta_n = -j(k_{cn}^2 - k^2)^{1/2} \quad (\text{for nonpropagating modes})$$

$$Z_0 = 120\pi. \quad (3)$$

The equivalent voltage of the n th waveguide mode excited by a known electric field can be found as

$$v_n = \int_S E \cdot E_{tn} dS. \quad (4)$$

In a similar fashion the equivalent current is found to be

$$i_n = \int_S H \cdot H_{tn} dS. \quad (5)$$

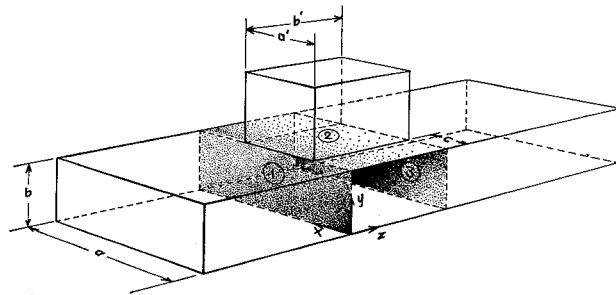


Fig. 1. T-junction with side arm of arbitrary cross section.

II. FORMAL ANALYSIS OF THE T-JUNCTION

In this analysis the T -junction boundary value problem is solved using equivalent-circuit concepts. In the T -junction of Fig. 1, terminal planes 1, 2, and 3 are shown positioned at the mouth of each waveguide forming the junction. At each terminal plane an infinite number of modes can exist and an equivalent current and voltage can be assigned to each mode. In Fig. 2 the equivalent network of the T -junction is shown with each equivalent current and voltage applied at a separate terminal pair. The equivalent network can be represented by an admittance matrix Y , which is three-fold infinite in size because an infinite number of modes can exist at each of the three terminal planes.

The procedure for analyzing the T -junction is now outlined in matrix notation. The matrix equation relating all the currents and voltages of all the modes at all the terminal planes is

$$i = Yv \quad (6)$$

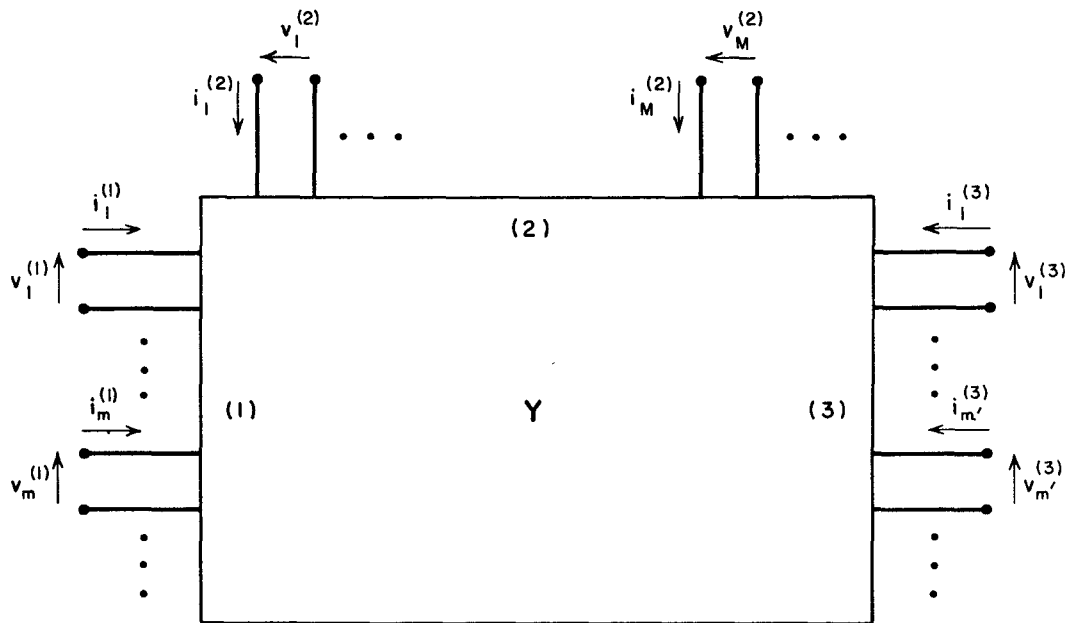
where i and v are current and voltage column matrices.

Before going any further it is convenient to define two special matrices:

$$A = \begin{pmatrix} 0 & & 0 \\ & \ddots & \\ & 1 & \\ & & 1 \\ 0 & & & \ddots & \ddots \end{pmatrix},$$

$$B = \begin{pmatrix} 1 & & 0 \\ & \ddots & \\ & 1 & \\ & & 1 \\ 0 & & & 0 & \end{pmatrix}. \quad (7)$$

Matrices A and B have null elements except on the lower and upper diagonal, respectively, where unit elements appear. The dividing point is chosen so that all the unit diagonal elements of B pertain to propagating modes and those of A

Fig. 2. Equivalent network of *T*-junction.

pertain to cutoff modes. The sum of matrices A and B equals the unit matrix. Equation (6) can now be written

$$i = YAv + YBv. \quad (8)$$

All cutoff modes are to be terminated in their respective wave impedances. Physically this means that the waveguides should be uniform near the junction so that the fields of the cutoff modes may attenuate to a small amplitude without perturbation. A terminating impedance matrix Z is defined as a matrix with the lower diagonal containing the negative of the wave impedance for all cutoff modes. The rest of the elements in the terminating impedance matrix are equal to zero. The negative of the wave impedance correctly terminates each cutoff mode because the positive current and voltage are chosen at a terminal in a direction representing positive power flow into the terminal. The termination of each cutoff mode in its respective wave impedance is expressed by the matrix equation

$$Av = Zi \quad (9)$$

where Z is the terminating impedance matrix.

By substituting (9) into (8) and transposing the resulting term we have

$$(1 - YZ)i = YBv \quad (10)$$

where 1 is the unit matrix. Premultiplying both sides of (10) by $B(1 - YZ)^{-1}$ we have

$$Bi = B(1 - YZ)^{-1}YBv = Y'v \quad (11)$$

which is the final form desired. Here $Y' = B(1 - YZ)^{-1}YB$ is the desired equivalent admittance matrix relating only the propagating modes to each other. Now the problem is reduced to finding Y , taking the inverse of $(1 - YZ)$, and premultiplying the result into Y .

III. CALCULATION OF THE INFINITE ADMITTANCE MATRIX

The steps outlined in Section II are now followed leading to a calculation of the equivalent admittance matrix Y' by first calculating the infinite admittance matrix Y . The admittance element Y_{mn} , where the indexes m and n go over all modes in all joining waveguides, can be calculated by applying an equivalent unit voltage at terminal n and short circuits at all other terminals, and by finding the equivalent current flowing at terminal m . For the *T*-junction of Fig. 1 the procedure is as follows. Assume, for example, that the index n of Y_{mn} represents a mode in waveguide 1. The requirement that all other modes be short circuited at all their reference planes means that all the equivalent voltages at terminal planes 2 and 3 are equal to zero. According to (1) then, the transverse electric field is zero at terminal planes 2 and 3. Thus, an electric wall can be placed at terminal planes 2 and 3. Looking into terminal plane 1, we see a length of uniform waveguide shorted at a distance b' from the input. The magnetic field H_n inside the shorted waveguide due to application of a unit voltage in mode n at terminal plane 1 is easily calculated. The admittance element Y_{mn} , being equal to the current at terminal m due to the excitation of the magnetic field H_n , using (5) is

$$Y_{mn} = \int_{S_m} \pm H_{tm} \cdot H_n dS. \quad (12)$$

The correct sign for H_{tm} must be chosen depending on the terminal plane. If the direction of positive power flow is into the junction according to the coordinate system, then the positive sign is chosen; otherwise the negative sign is chosen.

$$\begin{aligned}
 \left(\begin{array}{c} \text{TE}_{MN^{(2)}} \\ \text{TM} \end{array} \mid Y \mid \begin{array}{c} \text{TE}_{mn^{(1)}} \\ \text{TM} \end{array} \right) &= \frac{j Y_0 \epsilon_{MN} \epsilon_{mn} (-)^n \left[(-)^{M+1} \sin \frac{m\pi}{a} (a' + c) + \sin \frac{m\pi}{a} c \right]}{k_{c_{MN^{(2)}}} k_{c_{mn^{(1)}}} \sqrt{aa'bb'} \left(\frac{N^2\pi^2}{b'^2} - \beta_{mn^{(1)}}^2 \right) \left(\frac{M^2\pi^2}{a'^2} - \frac{m^2\pi^2}{a^2} \right)} \\
 &\cdot \begin{array}{c} \text{TE}_{mn^{(1)}} \\ \text{TM}_{MN^{(2)}} \end{array} \left| \begin{array}{c} \frac{m\pi}{a} \frac{1}{k} \left[k_{c_{MN^{(2)}}}^2 k_{c_{mn^{(1)}}}^2 - k^2 \frac{M^2\pi^2}{a'^2} \right] \\ k \frac{m\pi}{a} \frac{N\pi}{b'} \frac{M\pi}{a'} \end{array} \right| \begin{array}{c} \text{TM}_{mn^{(1)}} \\ \frac{-k}{n\pi} \frac{M^2\pi^2}{a'^2} \frac{n\pi}{b} \\ k \frac{n\pi}{b} \frac{N\pi}{b'} \frac{M\pi}{a'} \end{array} \end{aligned} \quad (16a)$$

The self-admittance elements at terminal plane 1 are equal to the admittances of a short-circuited waveguide.

$$\begin{aligned}
 \left(\begin{array}{c} \text{TE}_{m'n^{(1)}} \\ \text{TM} \end{array} \mid Y \mid \begin{array}{c} \text{TE}_{mn^{(1)}} \\ \text{TM} \end{array} \right) &= - \left(\begin{array}{c} \text{TE}_{m'n'} \\ \text{TM} \end{array} \mid \delta \mid \begin{array}{c} \text{TE}_{mn} \\ \text{TM} \end{array} \right) j Y_0 \\
 &\cdot \left\{ \begin{array}{c} \beta_{mn^{(1)}}/k \\ k/\beta_{mn^{(1)}} \end{array} \right\} \cot \beta_{mn^{(1)}} b', \quad (13)
 \end{aligned}$$

where

$$\left(\begin{array}{c} \text{TE}_{mn} \\ \text{TM} \end{array} \mid \delta \mid \begin{array}{c} \text{TE}_{mn} \\ \text{TM} \end{array} \right) = \begin{cases} 1 & \text{if all to left and right of } \delta \text{ is equal} \\ 0 & \text{if not.} \end{cases}$$

Because of the symmetry of the *T*-junction, the self-admittance elements for terminal plane 3 are equal to the self-admittance elements of terminal 1 given in (13). The transfer admittance element referring terminal planes 1-3 is found to be the transfer admittance of a uniform length of waveguide excited with one mode as follows:

$$\begin{aligned}
 \left(\begin{array}{c} \text{TE}_{m'n^{(3)}} \\ \text{TM} \end{array} \mid Y \mid \begin{array}{c} \text{TE}_{mn^{(1)}} \\ \text{TM} \end{array} \right) &= j Y_0 \left\{ \begin{array}{c} \beta_{mn^{(1)}}/k \\ k/\beta_{mn^{(1)}} \end{array} \right\} \\
 &\cdot \csc [\beta_{mn^{(1)}} b'] \left(\begin{array}{c} \text{TE}_{m'n'} \\ \text{TM} \end{array} \mid \delta \mid \begin{array}{c} \text{TE}_{mn} \\ \text{TM} \end{array} \right). \quad (14)
 \end{aligned}$$

To calculate the transfer admittance between terminal planes 1 and 2, (12) is used retaining the negative sign

$$\begin{aligned}
 \left(\begin{array}{c} \text{TE}_{MN^{(2)}} \\ \text{TM} \end{array} \mid Y \mid \begin{array}{c} \text{TE}_{mn^{(1)}} \\ \text{TM} \end{array} \right) &= - \int_c^{a'+c} dx \int_0^{b'} dz H_{t\text{TE}_{MN^{(2)}}} (z, x) \\
 &\cdot H_{\text{TE}_{mn^{(1)}}} (x, b, z), \quad (15)
 \end{aligned}$$

where

$$H_{\text{TE}_{mn}}$$

is the magnetic field excited inside the cavity by the application of unit voltage at terminal plane 1. The following results when the integrals are evaluated:

where

$$\epsilon_{mn} = \sqrt{2} \sqrt{2 - \delta_{m0} - \delta_{n0}}.$$

Equation (16a) is interpreted as follows: if the transfer admittance between two TE modes is desired, then use the upper left factor of the two-by-two lattice; if the transfer admittance between two TM modes is desired, then use the lower right factor of the lattice. The transfer admittance between a TE and TM mode is found by using the lower, left or upper right factor of the lattice. Equation (16a) is valid for all modes except those where both *M* and *m* are zero, in which case (16a) is seen to be indeterminant. The following is valid when both *M* and *m* are zero.

$$\begin{aligned}
 \left(\begin{array}{c} \text{TE}_{0N^{(2)}} \\ \text{TM} \end{array} \mid Y \mid \begin{array}{c} \text{TE}_{0n^{(1)}} \\ \text{TM} \end{array} \right) &= \frac{j Y_0 2(-)^n a' \frac{N\pi}{b'} \frac{n\pi}{b}}{k \sqrt{aa'bb'} \left(\frac{N^2\pi^2}{b'^2} - \beta_{0n^{(1)}}^2 \right)} \\
 &\quad (M = m = 0). \quad (16b)
 \end{aligned}$$

The symmetrical admittance element to (16) can be calculated by applying unit voltage in the mode at terminal plane 2, with electric walls at terminal planes 1 and 3. The typical case is shown in Fig. 3 in which unit voltage is applied in the $\text{TE}_{10^{(2)}}$ mode at terminal plane 2, and electric walls are placed at terminal planes 1 and 3. An *E*-field is applied in an aperture of smaller cross section than the cross section of the attached waveguide cavity, and an infinite number of waveguide modes propagating in *y*-dimension are excited by the applied *E*-field. After making the required calculations, it is found that the symmetric admittance elements are equal, as required by reciprocity.

According to (12) the self-admittance elements at terminal plane 2 are

$$\begin{aligned}
 \left(\begin{array}{c} \text{TE}_{M'N^{(2)}} \\ \text{TM} \end{array} \mid Y \mid \begin{array}{c} \text{TE}_{MN^{(2)}} \\ \text{TM} \end{array} \right) &= - \int_c^{a'+c} dx \int_0^{b'} dz H_{t\text{TE}_{M'N^{(2)}}} (z, x) \\
 &\cdot H_{\text{TE}_{MN^{(2)}}} (x, b, z), \quad (17)
 \end{aligned}$$

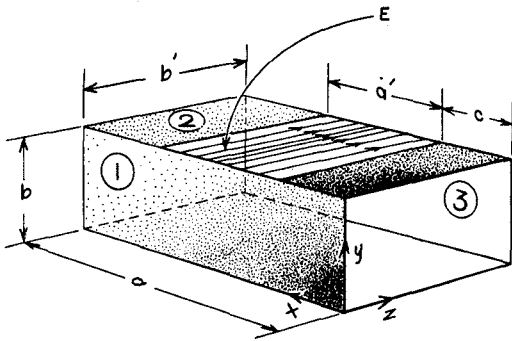


Fig. 3. T-junction with TE_{10} mode excited in side waveguide aperture and electric walls at terminal planes 1 and 3.

where

$$H_{TM}^{TE_{MN^{(2)}}}$$

(x, b, z) is the H -field excited in the waveguide cavity of Fig. 3 due to application of unit voltage at terminal plane 2 in the waveguide mode

$$TE_{MN^{(2)}}.$$

$$TM$$

Evaluating the integrals of (17), and after some algebra, the following results:

The calculation of the transfer admittance elements between terminal planes 2 and 3 follows steps very similar to the steps leading to (14). The result as expected from the symmetry of the junction is the same as (14) except for the sign

$$\begin{aligned} \left(\begin{matrix} TE_{mn^{(3)}} \\ TM \end{matrix} \mid Y \mid \begin{matrix} TE_{MN^{(2)}} \\ TM \end{matrix} \right) &= \left(\begin{matrix} TE_{MN^{(2)}} \\ TM \end{matrix} \mid Y \mid \begin{matrix} TE_{mn^{(3)}} \\ TM \end{matrix} \right) \\ &= (-)^{N+1} \left(\begin{matrix} TE_{mn^{(1)}} \\ TM \end{matrix} \mid Y \mid \begin{matrix} TE_{MN^{(2)}} \\ TM \end{matrix} \right). \end{aligned} \quad (20)$$

IV. NUMERICAL CALCULATIONS

In order to check the calculations presented in this paper with existing theoretical calculations and experimental results, some calculations have been made for the T -junction with common side walls when $a' = a$. These calculations are compared to the calculations and experimental values determined by Allanson, Cooper, and Cowling [6] for an E -plane T -junction. In this junction the dimensions are as follows: $a/b = a'/b' = 2$, and it is assumed that the TE_{10} mode with the E -field polarized perpendicular to the x -coordinate is the only mode that can propagate in each of the waveguides.

$$\begin{aligned} \left(\begin{matrix} TE_{M'N'^{(2)}} \\ TM \end{matrix} \mid Y \mid \begin{matrix} TE_{MN^{(2)}} \\ TM \end{matrix} \right) &= -jY_0 \frac{\epsilon_{M'N'}\epsilon_{MN}\delta_{NN'}}{(2 - \delta_{N0})^2 k_{c_{MN^{(2)}}} k_{c_{M'N'^{(2)}}} a a' k} \cdot \sum_{p=1}^{\infty} \frac{\epsilon_{pN}^2 \cot \beta_{pN^{(0)}} b}{\beta_{pN^{(0)}}} \\ &\quad \left[(-)^{M+1} \sin \frac{p\pi}{a} (a' + c) + \sin \frac{p\pi}{a} c \right] \left[(-)^{M+1} \sin \frac{p\pi}{a} (a' + c) + \sin \frac{p\pi}{a} c \right] \\ &\quad \left[\frac{M'^2 \pi^2}{a'^2} - \frac{p^2 \pi^2}{a^2} \right] \left[\frac{M^2 \pi^2}{a'^2} - \frac{p^2 \pi^2}{a^2} \right] \\ &\quad \begin{matrix} TE_{MN^{(2)}} & TM_{MN^{(2)}} \end{matrix} \quad (18) \\ &\quad \begin{matrix} TE_{M'N'^{(2)}} \\ TM_{M'N'^{(2)}} \end{matrix} \left[\begin{matrix} k^2 \left(\frac{p^2 \pi^2}{a^2} \frac{N^2 \pi^2}{b'^2} + \frac{M^2 \pi^2}{a'^2} \frac{M'^2 \pi^2}{a'^2} \right) - \frac{p^2 \pi^2}{a^2} k_{c_{M'N'^{(2)}}}^2 k_{c_{MN^{(2)}}}^2 \\ -k^2 \frac{N\pi}{b'} \frac{M'\pi}{a'} \left(\frac{M^2 \pi^2}{a'^2} - \frac{p^2 \pi^2}{a^2} \right) \end{matrix} \right] \left[\begin{matrix} -k^2 \frac{N\pi}{b'} \frac{M\pi}{a'} \left(\frac{M'^2 \pi^2}{a'^2} - \frac{p^2 \pi^2}{a^2} \right) \\ (1 - \delta_{N0}) \frac{M'\pi}{a'} \frac{M\pi}{a'} k^2 k_{c_{pN^{(0)}}}^2 \end{matrix} \right] \\ &\quad -jY_0 \delta_{M0} \delta_{M'0} \delta_{NN'} \frac{a'}{k} \frac{a'}{a} \cot \beta_{0N^{(0)}} b. \end{aligned}$$

If in the above expression we let c approach zero and let a' approach a , then (18) simplifies to

$$\begin{aligned} \left(\begin{matrix} TE_{M'N'^{(2)}} \\ TM \end{matrix} \mid Y \mid \begin{matrix} TE_{MN^{(2)}} \\ TM \end{matrix} \right) &= - \left(\begin{matrix} TE_{M'N'} \\ TM \end{matrix} \mid \delta \mid \begin{matrix} TE_{MN} \\ TM \end{matrix} \right) jY_0 \\ &\quad \cdot \left\{ \frac{\beta_{MN^{(2)}}/k}{k/\beta_{MN^{(2)}}} \right\} \cot \beta_{MN^{(2)}} b. \end{aligned} \quad (19)$$

The calculated equivalent admittance parameters of the E -plane T -junction are shown in Table I. These parameters were calculated by considering the first six cutoff modes in each waveguide forming the junction and are estimated to be accurate to within one percent.

The calculated positions of the reference planes are tabulated in Table II along with the calculated and measured values found by Allanson, Cooper, and Cowling. The agreement is seen to be excellent, and it can be concluded that the method of analysis presented here is verified by independent theoretical and experimental results.

TABLE I
EQUIVALENT ADMITTANCE PARAMETERS OF *E*-PLANE
T-JUNCTION FOR $a/b = a/b' = 2$

b/λ_g	Y_{11}'/Y_0	Y_{12}'/Y_0	Y_{13}'/Y_0	Y_{22}'/Y_0
0.05	-j0.606	j0.624	j0.633	-j0.608
0.15	-j0.396	j0.544	j0.618	-j0.414
0.25	-j0.067	j0.446	j0.651	-j0.119
0.30	j0.142	j0.402	j0.714	-j0.061
0.35	j0.410	j0.362	j0.843	j0.279
0.45	j1.725	j0.291	j1.896	j1.197
0.49998	j192.3	j0.255	j192.4	j102.1

TABLE II

CALCULATED REFERENCE PLANES OF *E*-PLANE *T*-JUNCTION FOR $a/b = a/b' = 2$ COMPARED TO THOSE MEASURED AND CALCULATED BY ALLANSON, COOPER, AND COWLING (ACC)

b/λ_g	p_1/λ_g	p_2/λ_g	Calculated by ACC		Measured by ACC	
			p_1/λ_g	p_2/λ_g	p_1/λ_g	p_2/λ_g
0.05	0.254	0.244	0.254	0.244	—	—
0.15	0.260	0.230	0.261	0.231	—	—
0.25	0.265	0.209	0.266	0.210	—	—
0.30	0.266	0.193	0.267	0.194	—	—
0.35	0.267	0.172	0.267	0.173	—	—
0.45	0.263	0.098	0.263	0.098	—	—
0.49998	0.250	0.001	—	—	—	—
0.50	0.250	0.000	0.250	0.000	—	—
0.198	—	—	0.263	0.221	0.268	0.228
0.303	—	—	0.266	0.193	0.278	0.197
0.397	—	—	0.267	0.144	0.268	0.130
0.43	—	—	0.263	0.116	0.267	0.116

Numerical calculations of the equivalent admittance matrix Y' are now made for a particular *T*-junction of the type that is shown in Fig. 1. The side waveguide is assumed to be centered with respect to the broad wall of the through waveguide; and the dimensions (inches) of two standard waveguides are chosen as follows: $a = 1.372$, $b = 0.622$, $a' = 0.900$, $b' = 0.400$, and $c = 0.236$. Over the frequency range considered, the TE_{10} mode is the only mode that can propagate in each waveguide. Below the cutoff frequency of the side waveguide the *T*-junction is equivalent to a two-terminal-pair network, and above the cutoff frequency on the side waveguide the *T*-junction is equivalent to a three-terminal pair network.

The calculated values of the equivalent admittance parameters are plotted in Figs. 4 and 5. The first five modes below cutoff in each waveguide were considered in these calculations. It is estimated that the admittance parameters plotted in Figs. 4 and 5 are accurate to within about two percent.

The scattering matrix of this junction is plotted in Figs. 6 and 7. Note that $|S_{11}|$, which is the amplitude of the reflection coefficient seen at terminal 1 when matched loads are placed in waveguides 2 and 3, goes through unity at the cutoff frequency of the side waveguide. This is because the side waveguide is electrically in series with the through waveguide and because the wave impedance of the side

TABLE III

MEASURED AND THEORETICAL POSITIONS OF
REFERENCE PLANES FOR THE *T*-JUNCTION
 $a = 1.372$ inches, $b = 0.622$ inch, $c = 0.236$ inch,
 $a' = 0.900$ inch, $b' = 0.400$ inch

$\lambda/2a$	Measured		Theoretical	
	p_1/λ_{g1}	p_2/λ_{g2}	p_1/λ_{g1}	p_2/λ_{g2}
0.62	0.166	0.202	0.166	0.199
0.60	0.162	0.201	0.162	0.197
0.55	0.149	0.190	0.149	1.180
0.50	0.129	0.160	0.133	0.152
0.42	0.107	0.058	0.101	0.050

waveguide passes through infinity at the cutoff frequency of the side waveguide. Far below the cutoff frequency of the side waveguide, most of the power is transmitted past the junction. Just above the cutoff frequency of the side waveguide, power is strongly coupled into the side waveguide and very soon almost one-half of the power incident in the through waveguide is coupled into the side waveguide. Then as the frequency is increased, the coupling between the through and side waveguides decreases gradually to zero as the cutoff frequency of the TE_{11} and TM_{11} modes in the through waveguide is approached. At this cutoff frequency the other scattering coefficients approach either zero or one; this is to be expected because at their cutoff frequencies the TE_{11} and TM_{11} modes place infinite and zero impedance, respectively, across their respective terminals.

Experimental measurements of the electrical parameters of the *T*-junction were made in order to check the theoretical calculations. The reference plane positions were measured at several frequencies above the cutoff frequency of the side waveguide. The position of the reference planes so measured is shown in Table III with the theoretical values. The agreement between the measured and theoretical positions of the reference planes is seen to be quite good.

Measured values of reflection coefficient amplitude looking into terminal 1 are shown in Fig. 6 for frequencies less than the cutoff frequency of the side waveguide, in excellent agreement with the theoretical results.

Generally, the comparison between the experiment and theory is quite good and it can be concluded that the theory has been well verified by experimental measurements.

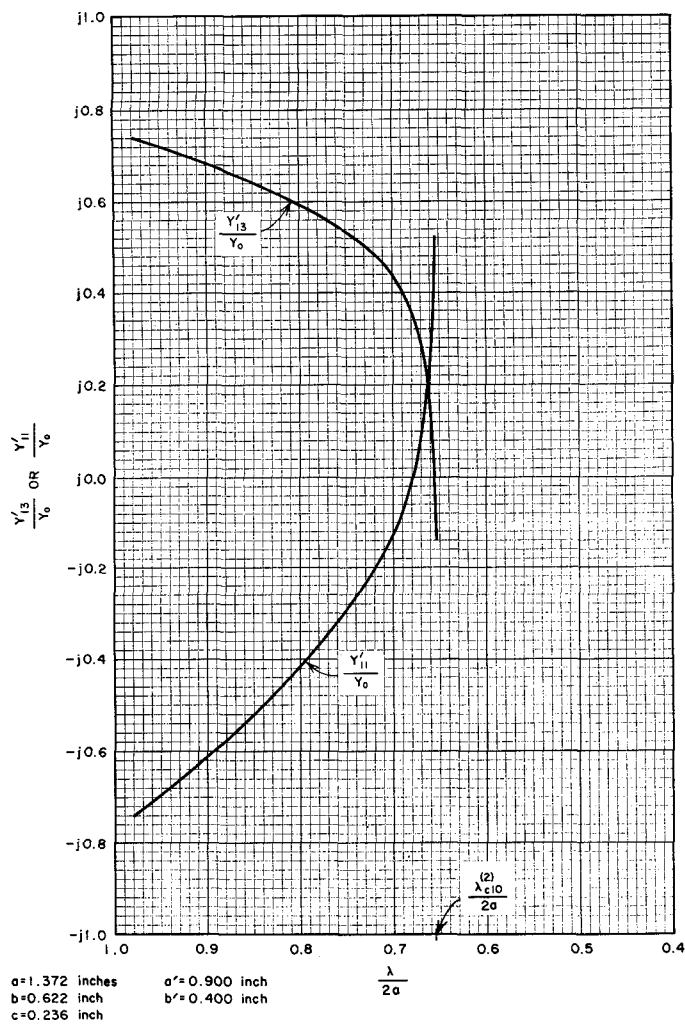


Fig. 4. Equivalent admittance parameters of the *T*-junction for frequencies below the cutoff frequency of the side waveguides.

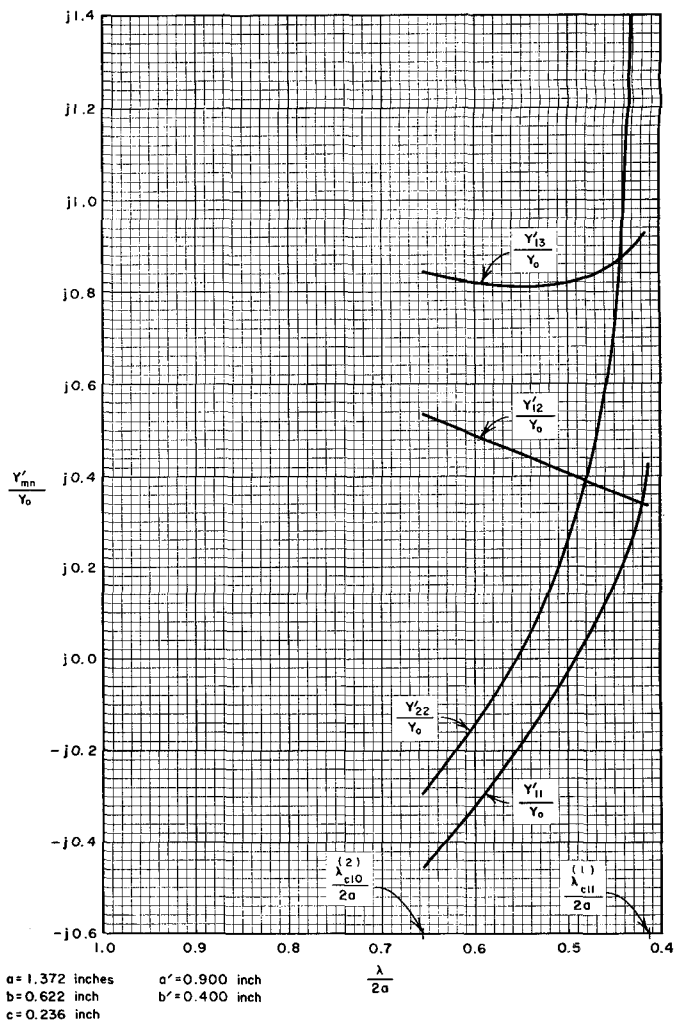


Fig. 5. Equivalent admittance parameters of the *T*-junction for frequencies above the cutoff frequency of the side waveguide.

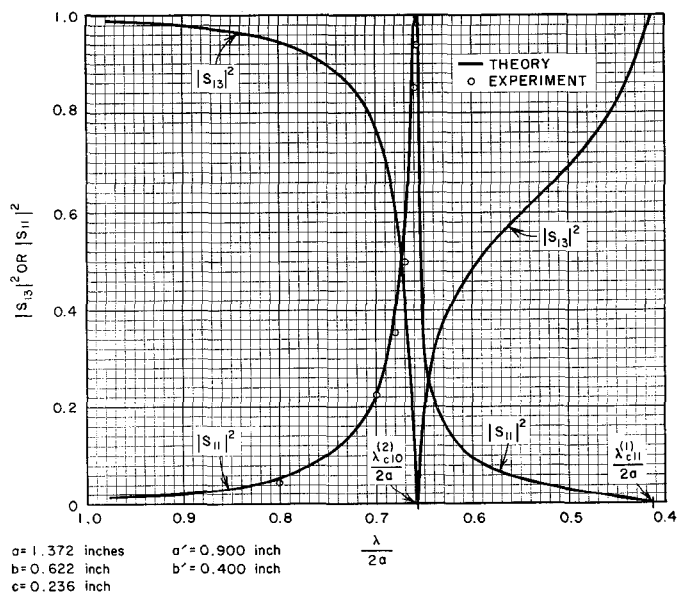


Fig. 6. Magnitude squared of the scattering parameters S_{11} and S_{13} of the *T*-junction.

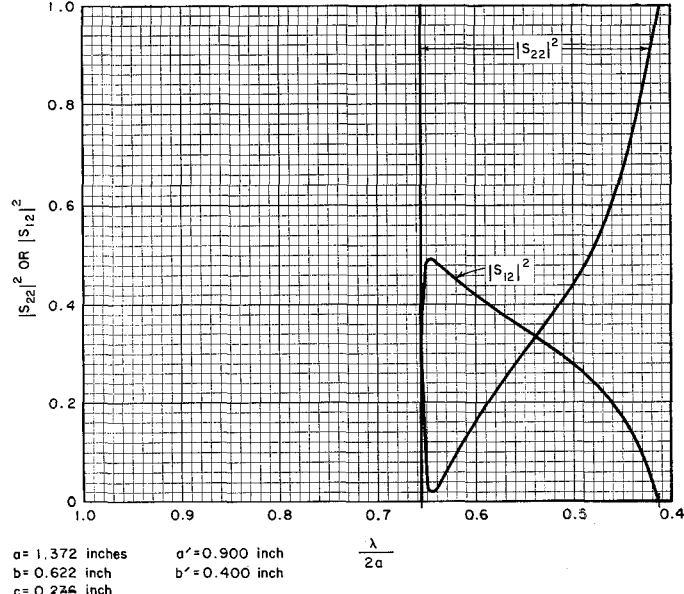


Fig. 7. Magnitude squared of the scattering parameters S_{12} and S_{22} of the *T*-junction.

V. CONCLUSIONS

An exact method has been developed for analyzing the electrical performance of a rectangular waveguide *T*-junction in which the cross-sectional dimensions of the side waveguide are different from the cross-sectional dimensions of the through waveguide. The formulas derived from the equivalent admittance matrix of the *T*-junction are general in that they apply to any right-angle rectangular waveguide *T*-junction; the side arm of the *T*-junction may be placed in any position in either the broad or narrow wall of the through waveguide provided that all waveguide surfaces are either at right angles or parallel to each other. This method requires the inversion of an infinite matrix; however, any desired accuracy can be obtained by considering a matrix of finite but sufficient size. Numerical calculations for two particular *T*-junctions showed that accuracies of about one-half percent can be achieved using matrices of reasonable size.

The method developed here is quite versatile and can be applied to the analysis of other rectangular waveguide discontinuities or junctions for which no exact analysis is presently available. Two examples of such junctions are the sudden change in both cross-sectional dimensions of a waveguide or a right-angle junction of more than three waveguides.

ACKNOWLEDGMENT

The author wishes to express his gratitude to Prof. E. T. Jaynes for his thoughtful and stimulating counsel during the course of this work. F. K. Tomlin programmed the digital computer to obtain numerical calculations.

REFERENCES

- [1] P. A. Rizzi, "Microwave filters utilizing the cutoff effect," *IRE Trans. on Microwave Theory and Techniques*, vol. MTT-4, pp. 36-40, January 1956.
- [2] V. Met, "Absorptive filters for microwave harmonic power," *Proc. IRE*, vol. 47, pp. 1762-1769, October 1959.
- [3] V. G. Price, R. H. Stone, and V. Met, "Harmonic suppression by leaky-wall waveguide filter," *IRE WESCON Rec.*, pt. 1, pp. 112-118, 1959.
- [4] E. M. T. Jones, S. B. Cohn, and E. D. Sharp, "Investigation of high-power filter techniques," Stanford Research Inst., Menlo Park, Calif., 1st Ann. Rept., SRI Project 2797, RADC-TR-60-79, March 1960.
- [5] C. G. Montgomery, R. H. Dicke, and E. M. Purcell, *Principles of Microwave Circuits*, M.I.T. Radiation Lab. Series, vol. 8. New York: McGraw-Hill, 1951.
- [6] J. T. Allanson, R. Cooper, and T. G. Cowling, "The theory and experimental behavior of right-angled junctions in rectangular-section waveguides," *J.IEE (London)*, vol. 93, pt. III, pp. 177-187, 1946.